New Insights in Chemical Reactivity by Means of Electron Pairing Analysis

Jordi Poater, Miquel Solà, Miquel Duran, and Xavier Fradera*,†

Institut de Química Computacional, Universitat de Girona, 17071 Girona, Catalunya, Spain

Received: October 5, 2000; In Final Form: December 11, 2000

According to the Lewis model, valence electrons in closed-shell atoms and molecules can be arranged into pairs of electrons shared between bonded atoms and lone pairs that belong to a single atom. Within this scheme, ionic bonding arises from the transfer of electrons between atoms, while covalent bonding is related to the sharing of electrons between atoms. Over the years, this simple model has proven to be extremely useful for the description of the bonding patterns in many molecules, and to describe the electronic rearrangements taking place during chemical reactions. However, a physically accurate description of the electron pairing in atoms and molecules has to be based on the electron-pair density. Within the theory of atoms in molecules, one can define atomic localization and delocalization indices which describe the intra- and interatomic distribution of the electron pairs in a molecule. Therefore, these indices can be considered as a physically sound and numerically accurate extension of the Lewis model. In this paper, we use localization and delocalization indices to study the electron-pair reorganization taking place in five different reactions: two intramolecular rearrangements, a nucleophilic substitution, an electrophilic addition, and a Diels−Alder cycloaddition. For each reaction, we perform a comparative analysis of the electron-pairing patterns in reactants, transition states, and products. The evolution of electron-pairing along the reaction path is also studied. In all cases, the use of localization and delocalization indices provides useful insights on the electronic rearrangements taking place during the reactions.

Introduction

The basic assumption of the Lewis model is to consider that valence electrons in atoms and molecules are arranged in pairs of electrons of different spin, which can be classified as shared or lone pairs.[1] Accordingly, covalent bonds are formed by sharing electron pairs between atoms, while ionic bonds are associated with the transfer of electrons from electropositive to electronegative elements. Between the two extremes of covalent and ionic bonding, one can have different degrees of polar bonding. The Lewis model has become de facto the basis for the chemical language, and reasonings based on this simple model are still widely used for understanding the electron reorganization processes taking place in chemical reactions.

To study the patterns of electron pairing in atoms or molecules from a physical point of view, one has to resort to the electron-pair density.[2] The formation of (α,β) pairs of electrons is due to the antisymmetry of the electronic wave function with respect to the interchange of the space−spin coordinates of any pair of electrons. This is a consequence of the Pauli exclusion principle, which states that two same-spin electrons cannot be at the same time at the same position of space. In practice, this creates a Fermi or exchange hole density function around each electron; that is, there is a region surrounding each electron where the probability of having a second electron with the same spin is very low. The Fermi hole around each electron, which integrates to −1 throughout all the space, accounts for the pairing of electrons of different spin.[3,4]

Fermi correlation between same-spin electrons is often sufficient to get a reasonable description of the electronic structure of atoms and molecules: this is the case of the Hartree−Fock (HF) approximation. However, post-HF methods, such as Møller−Plesset (MP) or configuration interaction (CI), consider also Coulomb correlation between electrons of different spin. In this case, one can refer to the corresponding hole density function as the exchange-correlation hole.

At any level of theory, by means of the one and two-electron density functions, $\rho^{\sigma}(\mathrm{r})$ and $\Gamma^{\sigma\sigma'}(\mathbf{r}_1,\mathbf{r}_2)$, respectively, one can define a function, $f^{\sigma\sigma'}(\mathbf{r}_1,\mathbf{r}_2)$, as[2,5]

$$f^{\sigma\sigma'}(\mathbf{r}_1,\mathbf{r}_2) = 2\Gamma^{\sigma\sigma'}(\mathbf{r}_1,\mathbf{r}_2) - \rho^{\sigma}(\mathbf{r}_1)\rho^{\sigma'}(\mathbf{r}_2) \qquad (1)$$

where σ and σ' are the spin coordinates (α or β) of the electrons and $f^{\sigma\sigma}(\mathbf{r}_1,\mathbf{r}_2)$ is the Fermi or exchange density, while $f^{\sigma\sigma'}(\mathbf{r}_1,\mathbf{r}_2)$, with $\sigma \neq \sigma'$, is the Coulomb density. At the HF level of theory, $f^{\alpha\beta}(\mathbf{r}_1,\mathbf{r}_2) = 0$. The total exchange-correlation density is defined by

$$f(\mathrm{r}_1,\mathbf{r}_2) = f^{\alpha\alpha}(\mathbf{r}_1,\mathbf{r}_2) + f^{\alpha\beta}(\mathbf{r}_1,\mathbf{r}_2) + f^{\beta\alpha}(\mathbf{r}_1,\mathbf{r}_2) + f^{\beta\beta}(\mathbf{r}_1,\mathbf{r}_2) \qquad (2)$$

with

$$\int f(\mathbf{r}_1,\mathbf{r}_2)\, \mathrm{d}\mathbf{r}_1 \mathrm{d}\mathbf{r}_2 = -N \qquad (3)$$

The $f^{\sigma\sigma'}(\mathbf{r}_1,\mathbf{r}_2)$ function can be used to define the Fermi ($\sigma = \sigma'$) or Coulomb ($\sigma \neq \sigma'$) hole density functions as

$$h^{\sigma\sigma'}(\mathbf{r}_1,\mathbf{r}_2) = \frac{f^{\sigma\sigma}(\mathbf{r}_1,\mathbf{r}_2)}{\rho^{\sigma}(\mathbf{r}_1)} = \frac{2\Gamma^{\sigma\sigma}(\mathbf{r}_1,\mathbf{r}_2)}{\rho^{\sigma}(\mathbf{r}_1)} - \rho^{\sigma'}(\mathbf{r}_2)$$

$$\int h^{\sigma\sigma}(\mathbf{r}_1,\mathbf{r}_2)\, \mathrm{d}\mathbf{r}_2 = -1; \quad h^{\sigma\sigma}(\mathbf{r}_1,\mathbf{r}_2)\, \mathrm{d}\mathbf{r}_2 = 0 \qquad (4)$$

where $\mathbf{r}_1$ and σ are the spatial and spin coordinates, respectively,

* Corresponding author. E-mail: xavier@iqc.udg.es.
† Present address: Departament de Físicoquímica, Facultat de Farmàcia, Universitat de Barcelona, Avda. Diagonal s/n, 08028 Barcelona, Spain.

10.1021/jp003655v CCC: $20.00
Published on Web 02/10/2001

corresponding to the reference electron, whereas coordinate $\mathbf{r}_2$ shows in which regions of real space takes place the exclusion of electrons with spin σ'. Pictures of hole density functions have been used to illustrate how electrons are more or less localized in different regions of real space.[3,4] For instance, Fermi hole functions, $h^{\sigma\sigma}(\mathbf{r}_1,\mathbf{r}_2)$, show that core electrons are usually highly localized around atomic nuclei and are not correlated with valence electrons. On the contrary, when one considers a reference electron at a point between two atoms forming a covalent bond, one finds that the corresponding hole density is spread along a large region. Furthermore, the atoms in molecules theory (AIM)[6] allows to define weighted atomic holes which do not depend on the position of a reference electron, but rather on the electron density associated to an atom.[7] Moreover, plots of the Laplacian of the electron density, $\nabla^2\rho(\mathbf{r})$,[6] or the electron localization function (ELF)[8] also reveal regions of maximal electron pairing, which can be usually associated to core, valence lone pair, and valence shared electrons.

Pictures of the $h^{\sigma\sigma'}(\mathbf{r}_1,\mathbf{r}_2)$, $\nabla^2\rho(\mathbf{r})$, or ELF functions provide a convenient way to obtain visual information on the electron localization patterns at different points of real space. However, they do not yield quantitative information on the actual degree of electron pairing or correlation within atoms or between atoms. An alternative quantitative approach is the definition of atomic localization and delocalization indices,[9] using the atoms defined in the AIM theory.[6] According to this theory, atomic basins are regions in real space bounded by zero-flux surfaces in the one-electron density. Thus, one can obtain an atomic localization index, λ(A), by integrating the Fermi or exchange-correlation density within the atomic basin of atom A

$$\lambda(\mathrm{A}) = -\int_{\mathrm{A}} f(\mathbf{r}_1,\mathbf{r}_2)\, \mathrm{d}\mathbf{r}_1\mathrm{d}\mathbf{r}_2 \tag{5}$$

while an atomic delocalization index between a pair of atoms, δ(A,B), can be obtained by integrating the two electron coordinates in $f(\mathbf{r}_1,\mathbf{r}_2)$ over the atomic basins of A and B, respectively

$$\delta(\mathrm{A,B}) = -\int_{\mathbf{A}}\int_{\mathbf{B}} \boldsymbol{f}(\mathbf{r}_1,\mathbf{r}_2)\, \mathrm{d}\mathbf{r}_1\mathrm{d}\mathbf{r}_2 - \int_{\mathrm{B}}\int_{\mathrm{A}} f(\mathbf{r}_1,\mathbf{r}_2)\, \mathrm{d}\mathbf{r}_1\mathrm{d}\mathbf{r}_2 = -2\int_{\mathrm{A}}\int_{\mathrm{B}} f(\mathbf{r}_1,\mathbf{r}_2)\, \mathrm{d}\mathbf{r}_1\mathrm{d}\mathbf{r}_2 \tag{6}$$

λ(A) gives the number of electrons that are localized in A. In the limit of an atom with totally closed-shell interactions with its neighbors, λ(A) should approach the atomic electron population, N(A). This ideal case corresponds to a situation where there is no exchange or correlation between electrons in A and electrons in other atoms. In real systems, there is always some degree of electron delocalization between pairs of neighboring atoms. Maximal electron delocalization takes place for open-shell (covalent) homonuclear interactions. Thus, for a pair of electrons shared between two identical atoms, the maximal possible delocalization corresponds to $\delta(\mathrm{A,A}') = 1$, with $\lambda(\mathrm{A}) = \lambda(\mathrm{A}') = 0.5$, and the number of electron pairs shared between the atoms is equivalent to the delocalization index. This is the case of the H_2 molecule at the HF level of theory. However, for electrons shared between different atoms, or beyond the HF approximation, one can no longer consider that δ(A,B) yields the number of electron pairs involved in the bond. For instance, each of the electron pairs participating in the π_x and π_y bonds in CO is shared in the following way (at the HF level of theory): $\lambda(\mathrm{C}) = 0.04$, $\lambda(\mathrm{O}) = 1.50$, $\delta(\mathrm{C,O}) = 0.46$, revealing that these electron pairs are localized mainly on the O atom, with some part of the electron pair shared between both atoms and virtually no π electron density localized in C. Even though only approximately 0.5 π_x (or π_y) electrons are delocalized between C and O, there are indeed one π_x and one π_y electron pairs involved in the C−O bonding in this molecule. A similar reasoning applies to the σ density in this molecule.

Recently, localization and delocalization indices were calculated for a number of diatomic and polyatomic molecules, at the HF and CISD levels of theory.[9] It was found that the patterns of electron pairing predicted by means of the Lewis model were generally in good agreement with results obtained at the HF level of theory, especially for diatomic molecules. Indeed, the fact that the HF approximation does not consider Coulomb correlation overestimates the pairing of electrons of different spin. Taking into account Coulomb correlation at the CISD level yields results that are less in agreeement with the simple Lewis model, especially for covalent interactions, where interatomic delocalization decreases strongly, with respect to HF. Recently, Bader and Bayles[10] have used these indices to investigate the transferability of electron delocalization in methylene and silylene groups in hydrocarbons and oligosylanes, respectively, using the HF approximation. It is worth mentioning that at the SCF level, the delocalization indices in eq 6 reduce to Wiberg indices[11] if the exact integration over the atomic basins is replaced by the Mulliken-like approximation of the corresponding integrals. Using this approximation, Ponec and co-workers[12] have reported calculations of localization and delocalization indices at the semiempirical and HF levels of theory.

Furthermore, several authors have used the HF definitions of λ and δ (see below) with Kohn−Sham wave functions obtained with the B3LYP functional.[13,14] However, the HF-like pair density obtained from the Kohn−Sham determinant can be considered only as a first approximation to the real electron-pair density.[15] Therefore, one can expect DFT λ and δ values obtained in this way to be artificially close to the HF values.

In addition, several authors have proposed definitions closely related to the indices used in the present paper. For instance, Ángyán et al.[16] have defined valence and bond-order indices, and Fulton[17] has defined a sharing index. Both definitions are equivalent to the λ and δ indices used in this paper only at the HF level of theory. Cioslowski and Mixon[18] use an alternative expression to define a bond-order index which depends on a particular orbital localization procedure and is not invariant with respect to unitary transformations of the orbitals. Yamasaki and co-workers[19] have used the bond-order index definition in ref 16 to study bond orders in the transition states of some reactions and have performed a statistical analysis to determine the degree of correlation between bonds in a molecule. Finally, it has also been recently shown that electron populations obtained from integration of the one-electron density over bonding domains defined according to the ELF can be correlated to the delocalization indices used in the present paper, especially for nonpolar bonds.[14]

λ and δ calculations in ref 9 always refer to molecules at the energetic minimum of the potential energy hypersurface. However, one could also use localization and delocalization indices to study the electron pair reorganization taking place along a given reaction path. On one hand, bond breaking and formation processes have important consequences for the pairing of the electrons in the atoms involved in the reaction. On the other hand, electron pairing can be expected to remain nearly constant for the rest of atoms, unless long distance effects are important.

The aim of this paper is to investigate the electron pair changes taking place in five well-known reactions in the gas

phase. The idea of monitoring the course of the reaction by the value of bond orders or some other related bond indices has been applied in the past by several authors.[20,21] Our work differs from these earlier studies in that it replaces the previously used Wiberg indices or effective pair populations by the delocalization indices calculated within Bader's AIM theory. In particular, two intramolecular rearrangements involving H-transfer, a S_N2 nucleophilic substitution, an electrophilic addition, and a Diels−Alder cycloaddition have been studied. For all these reactions, atomic populations and localization indices were calculated for each atom, and delocalization indices for each pair of atoms, at several points along the reaction coordinate, paying special attention to the stationary points corresponding to reactants, products, and transition states.

Computational Methods

The electron-pair analysis was carried out for five different reactions: the CNH to HCN[21−25] and H_2SO to HSOH[24−26] intramolecular rearrangements, the S_N2 substitution of Cl by F in CH_3Cl,[27] the addition of hydrogen fluoride to ethene,[28] and the Diels−Alder cycloaddition of ethene to butadiene.[29,30] For all these reactions, HF wave functions and localization and delocalization indices were calculated for the optimized geometries corresponding to reactant, transition state (TS), and product, and for a number of points along the intrinsic reaction path (IRP) obtained using mass-weighted coordinates.[31] Meanwhile CISD calculations of localization and delocalization indices were carried out for the CISD-optimized geometries corresponding to reactant, transition state, and product of the two intramolecular rearrangement reactions and the electrophilic addition. Note that, for the Diels−Alder cycloaddition, the reactants do not correspond to a stable molecular complex; instead, they consist of two separate molecules. In this case, localization and delocalization indices were calculated separately for each of the reactant molecules, assuming that delocalization indices between atoms in the two molecules are exactly zero at long distance.

At the HF level, localization and delocalization indices can be calculated according to the following expressions

$$\lambda(\mathrm{A}) = -\sum_{i,j} (S_{ij}(\mathrm{A}))^2; \quad \delta(\mathrm{A,B}) = -2\sum_{i,j} S_{ij}(\mathrm{A})S_{ij}(\mathrm{B}) \qquad (7)$$

where $S_{ij}(\mathrm{A})$ corresponds to the overlap integral of the molecular orbitals i and j within the atomic basin of A. These values can be obtained by means of the Proaim program in the AIMPAC package.[32] At the CISD level, one must consider explicitly the matrix elements of the second-order density, $D_{\mu\nu\lambda\sigma}$, and the following expressions are obtained

$$\lambda(\mathrm{A}) = -\sum_{\mu,\nu,\lambda,\sigma} D_{\mu\nu\lambda\sigma}(S_{\mu\nu}(\mathrm{A}))^2;$$
$$\delta(\mathrm{A,B}) = -2\sum_{\mu,\nu,\lambda,\sigma} D_{\mu\nu\lambda\sigma}S_{\mu\nu}(\mathrm{A})S_{\lambda\sigma}(\mathrm{B}) \qquad (8)$$

The $D_{\mu\nu\lambda\sigma}$ matrix elements can be obtained from the GAMESS program,[33] after some minor modifications, while the atomic overlaps between basis functions, $S_{\mu\nu}(\mathrm{A})$, can be calculated from the $S_{ij}(\mathrm{A})$ overlaps.

The accuracy of the atomic integrations for a given molecule can be assessed by checking that both the summation of the atomic populations and the summation of all the λ and δ indices produce the number of electrons in the molecule. For most of the calculations reported in this paper, both summations yield the number of electrons with errors of less than 0.01 electrons. However, for some of the calculations, especially at the CISD level, the summation of the localization and delocalization indices produces errrors of ca. 0.05 electrons.

At the HF level, in some cases, one can split the λ and δ indices into contributions from molecular orbitals belonging to different symmetry species. For this partition to be possible, one needs all the overlaps over atomic basins between orbitals of different symmetry to be zero. This can be done easily for partitioning the indices into σ and π contributions for linear or planar molecules,[9] but may be not feasible or less accurate for molecules with more complex symmetries. When necessary, the separate contributions of different symmetry species to atomic populations, localization, and delocalization indices are specified.

The 6-31G* basis set[34] was used throughout, except for the S_N2 reaction, where diffuse s and sp functions were added to the hydrogen and heavy atoms, respectively (6-31++G* basis set). The programs Gaussian 98[35] and GAMESS[33] were used for the HF and CISD calculations, respectively. Location of critical points on the one-electron density and integrations of atomic properties were performed by means of the AIMPAC collection of programs.[32]

Results and Discussion

HF values of localization and delocalization indices for reactants, transition states, and products are presented for all the reactions, in Tables 1−5. Moreover, CISD values are also reported in Tables 1, 2, and 4. Scheme 1 depicts the HF geometries of the reactants, transition states, and products for all the reactions (when possible, CISD values have also been included). In all cases, reactants and products are defined as to make the reaction exothermic. The evolution of selected localization and delocalization indices along the IRP at the HF level is presented in Figures 1−5. The discussion of the results will be carried out separately for each reaction.

A. CNH → HCN Intramolecular Rearrangement. This is the simplest of the reactions studied, in terms of number of atoms, and will be used to illustrate in detail the methodological analysis performed. Table 1 gathers atomic populations and localization and delocalization indices for the reactant, TS, and product for this reaction, while Scheme 1 depicts the geometry of these structures, and Figure 1 shows the evolution of the three delocalization indices along the IRP. First of all, we will discuss the electronic differences between the CNH and HCN molecules at the HF level (see Table 1a). Second, the TS and the evolution of delocalization indices along the reaction path will be studied. Finally, we will use the CISD results (see Table 1b) to discuss the effect of Coulomb correlation on the electron pairing.

Atomic populations in CNH show a charge transfer from C and H toward N; i.e., the atomic populations for C, N, and H are 4.78, 8.80, and 0.42, which correspond to atomic charges of +1.22, −1.80, and +0.58, respectively. For HCN, the atomic charge in C is nearly the same as in CNH (+1.24) while the charges in N and H decrease in magnitude (−1.48 and +0.24, respectively), reflecting a higher polarity of the N−H bond in front of the C−H bond. An analysis of the σ and π contributions (π_x and π_y contributions are equivalent for linear molecules) to the atomic populations shows more differences between the CNH and HCN molecules. Thus, the CNH → HCN rearrangement leads to a decrease of the σ density in C (−0.53 e) and an increase in N (+0.20 e) and H (+0.33 e), while, at the same time, for each of the π_x and π_y electron pairs, there is a redistribution of 0.52 e from N to C. The π density within the

SCHEME 1: HF-Optimized Geometries for Reactants, Transition States, and Products of the Five Reactions Analyzed[a]

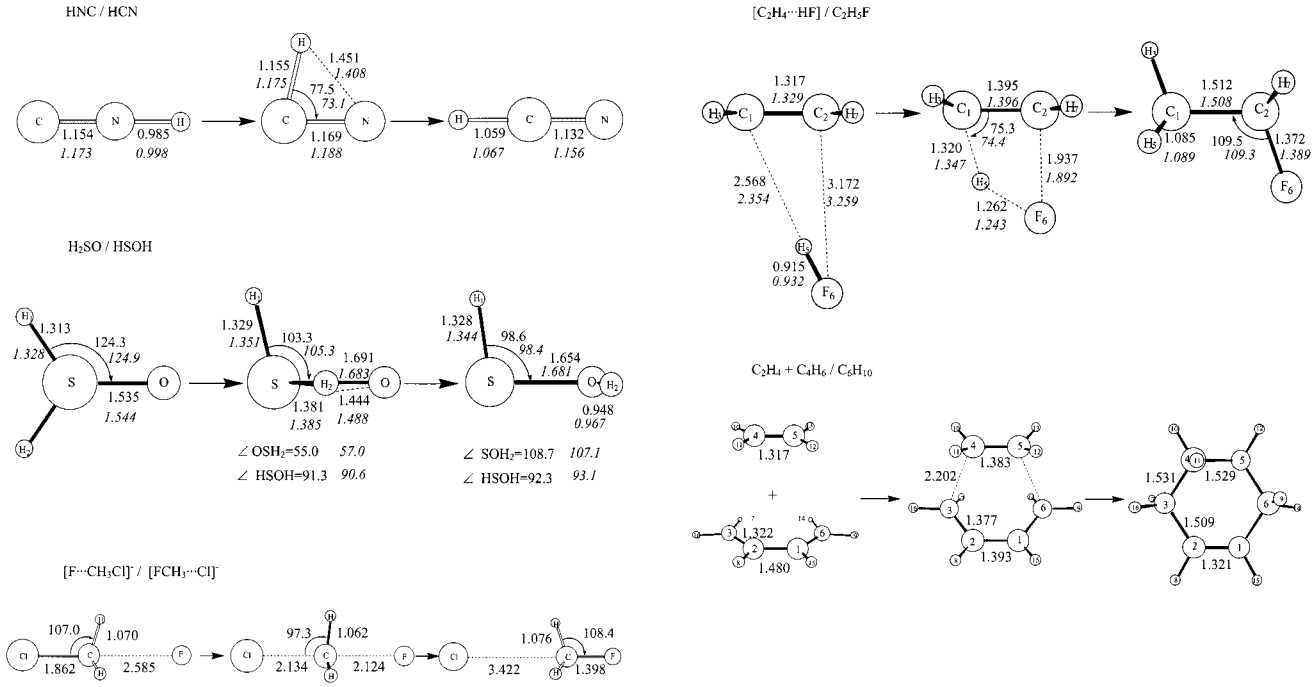

[a] Bond lengths are given in Å and angles in degrees. Values in italics refer to geometries obtained at the cisd level of theory.

TABLE 1: Atomic Populations (N), Localization (λ), and Delocalization (δ) Indices for the Reactant, Transition State, and Product of the CNH → HCN Intramolecular Rearrangement Reaction, Calculated at the HF/6-31G* and CISD/6-31G* Levels of Theory[a]

(a) HF/6-31G*

	reactant				TS			product			
	total	s	A′	π/A″	total	A′	A″	total	s	A′	π/A″
N(N)	8.803	5.461	8.803	3.342	8.352	6.764	1.588	8.481	5.664	8.481	2.817
N(C)	4.776	4.132	4.777	0.645	4.960	4.586	0.399	4.761	3.599	4.761	1.162
N(H)	0.421	0.408	0.421	0.013	0.683	0.668	0.014	0.758	0.737	0.758	0.021
λ(N)	7.635	4.843	6.239	1.396	7.181	5.920	1.261	7.323	5.339	6.331	0.992
λ(C)	3.927	3.823	3.875	0.052	3.791	3.712	0.079	3.191	2.853	3.022	0.169
λ(H)	0.083	0.083	0.083	0.000	0.206	0.206	0.000	0.271	0.271	0.271	0.000
δ(N,C)	1.679	0.601	1.140	0.539	1.861	1.230	0.631	2.242	0.605	1.424	0.818
δ(N,H)	0.656	0.634	0.645	0.011	0.477	0.454	0.022	0.074	0.044	0.059	0.015
δ(C,H)	0.020	0.016	0.018	0.002	0.473	0.468	0.006	0.900	0.887	0.894	0.006

(b) CISD/6-31G*

	reactant	TS	product
N(N)	8.614	8.258	8.249
N(C)	4.940	5.081	4.995
N(H)	0.446	0.661	0.756
λ(N)	7.559	7.283	7.299
λ(C)	4.178	4.121	3.685
λ(H)	0.119	0.239	0.315
δ(N,C)	1.490	1.515	1.819
δ(N,H)	0.619	0.445	0.081
δ(C,H)	0.034	0.411	0.800

[a] For the HF calculations, the separate contributions of orbitals belonging to different symmetry species are also presented.

H basin is very low (0.01 and 0.02 e for reactant and product, respectively).

According to the Lewis model, both CNH and HCN can be considered formally to have three pairs of electrons shared between the C and N atoms, and another electron pair shared between the H atom and one of the heavy atoms. However, the λ and δ indices exhibit significant differences in electron pairing between the two molecules. For instance, δ(C,H) in HCN (0.90) is larger than δ(N,H) in CNH (0.66), in agreement with the higher electronegativity of N in front of C. Accordingly, λ(H) is also much larger (0.27) for HCN than for CNH (0.08). On the contrary, CNH presents larger λ(N) and λ(C) values (7.63 and 3.93, respectively) than HCN (7.32 and 3.19, respectively). Finally, δ(N,C) is clearly smaller for CNH (1.68) than for HCN (2.24). Thus, it is clear that the C−N bond is more polar in CNH than in HCN.

It is also interesting to compare the values of the atomic localization indices to the associated atomic populations. For instance, the λ(H) values in the two molecules are quite small, and the ratio λ(H)/N(H) is of 20% and 36% in CNH and HCN, respectively, while the corresponding value for N is ca. 86% in the two molecules, and for C, 82% in CNH and 67% in HCN.

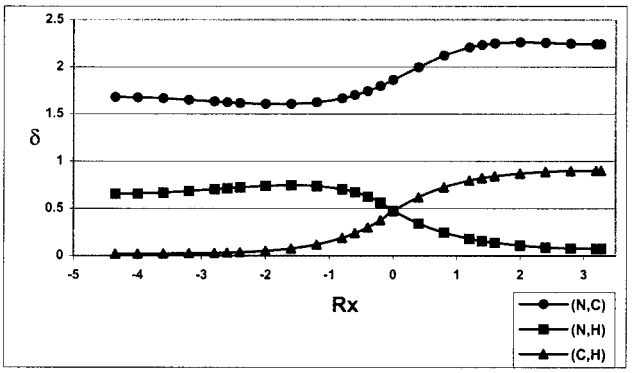

Figure 1. Evolution of the values of delocalization indices along the CNH → HCN rearrangement reaction, calculated at the HF/6-31G* level of theory. Negative and positive values of the reaction coordinate (R_x) correspond to reactant (CNH) and product (HCN), respectively. The TS is located at $R_x = 0$.

Thus, not only do electronegative atoms have more electrons in their basins, but also such electrons are more localized. Altogether, results in Table 1 point out that, compared to CNH, HCN presents less electron transfer between atoms, and a higher degree of electron sharing between bonded atoms.

Further insight on the electronic differences between reactants and products can be gained by analyzing the σ and π contributions to the atomic populations and indices. First of all, the σ density includes the contribution of the *core* electrons in C and N. Although the contributions of *core* and valence electrons cannot be separated strictly, one can assume that there is always one pair of *core* electrons on C and another on N, which are nearly uncorrelated to the rest of electrons in the molecule and do not play any role in the rearrangement reaction.[36] This leaves a total of six σ valence electrons, corresponding formally to two bonding pairs and one lone pair. Thus, the σ electronic rearrangement taking part in the reaction can be depicted schematically as

$$|C-N-H \rightarrow H-C-N|$$

According to this scheme, and assuming that the lone-pair electrons contribute mainly to λ^{σ}(C) in CNH, and to λ^{σ}(N) in HCN, one can predict that the rearrangement will involve an increase in λ^{σ}(N) and a decrease in λ^{σ}(C). This is actually confirmed by the numerical calculations, which reveal an increase of +0.50 in λ^{σ}(N) and a decrease of −0.97 in λ^{σ}(C) between reactant and product. However, λ^{σ}(N) is always larger than λ^{σ}(C), even for CNH, because the two bonded electron pairs are differently shared between C, N, and H, and because the lone pair is more localized in HCN than in CNH. Indeed, only the contribution of the σ density is relevant for λ and δ indices involving the H atom. Therefore, the changes in λ^{σ}(H), δ^{σ}(N,H) and δ^{σ}(C,H) are exactly those discussed above for the indices corresponding to the total density; i.e., the C−H electron pair in HCN is shared more evenly than the N−H pair in CNH. Interestingly, the value of δ^{σ}(N,C) remains almost constant (0.60 and 0.61, for CNH and HCN, respectively), revealing that the C−N σ electron pair is shared in the same way in the two molecules. This finding is in agreement with the results obtained by Rao using bond-order indices.[21]

The analysis of the π density is easier, because there is only one electron pair for each of the π_x and π_y symmetries, which are equivalent. Moreover, each of these electron pairs is shared only between C and N. For CNH, most of the π_x (or π_y) density is localized mainly within the N atom (1.40), whereas 0.54 π_x electrons are delocalized between C an N, and very little π_x density is localized on C (0.05). In contrast, for the HCN molecule, the π_x contributions to λ^{π}(N), λ^{π}(C), and δ^{π}(N,C) are 0.99, 0.17, and 0.82, respectively, showing that the π_x (and the π_y) electron pair is shared more evenly between C and N in the HCN molecule, compared to CNH. Thus, the separate analysis of the σ and π densities reveals that the differences in the covalent character of the C−N bond in the reactant and product molecules are due to changes in the localization of the π density.

Within the molecular orbital (MO) approximation used throughout this paper, the different polarities of the C−N bond in HCN and CNH can be rationalized by considering the effect of adding a proton to a CN^- molecule on the π MO's of this molecule. First of all, an analysis of the MO coefficients of the π_x orbital in CN^- shows that the contribution of the p_x atomic orbital (AO) of the N atom is larger than that of the p_x AO of the C atom. This is the result of the different energies of the p_x AO in C and N, the latter being significantly more stable. Adding a proton to the C atom to form the HCN molecule changes this situation, leading to a larger stabilization of the p_x AO of the C atom that is closer to the proton, and therefore, to a more even participation of the p_x AO of C and N to the π_x MO. In contrast, when the proton is added to the N atom to form the CNH molecule, it is the p_x AO of the N atom that is more stabilized, and the difference in the contributions of the two atoms to the π_x MO is increased with respect to CN^-. The same reasoning can be used for the π_y MO. Thus, the different contributions of N and C to the π orbitals in HCN and CNH account for the differences in the δ^{π}(N,C) values for these two molecules: for HCN, the π bond is formed by mixing AO of similar energy, leading to an even sharing of the π electron pairs between the two atoms. In contrast, for CNH, the contribution of the AO's in N is more important and, therefore, the π electron pair is more localized in the N atom.

Once the electronic structure of reactant and product has been analyzed, we will discuss the electronic features of the TS. In this structure, the three atoms are organized in a triangular shape, with H−C and H−N distances and HCN angle of 1.16 Å, 1.45 Å, and 77.5°, respectively (see Scheme 1). The delocalization index of H with each one of the heavy atoms is ca. 0.47. Although the values for λ(C) (3.79), λ(H) (0.21), and δ(N,C) (1.86) are intermediate between those of CNH and HCN, λ(N) is minimal at the TS (7.18). Since the TS has C_s symmetry, while the reactant and product molecules are linear, a comparison of different symmetry contributions to the localization and delocalization indices in the three structures can be performed by considering only the C_s symmetry elements, which are common to the three structures. Thus, Table 1 reports also the contributions of the 12 electrons belonging to the A′ symmetry species and the 2 electrons belonging to the A″ symmetry. Note that, for the linear molecules, the A″ symmetry species is equivalent to the π_x one, while the A′ symmetry collects the contributions from σ and π_y electrons, assuming that the molecule lies on the *yz* plane. In general, the comparison of the A′ and A″ contributions to the λ and δ indices of the three structures shows that, in both cases, the arrangement of the electrons in the TS is intermediate between the reactant and product. The only exception is for the A′ contribution to λ(N), which is minimal at the TS (5.92) with respect to the reactant (6.24) and product (6.33). This is the same trend found for the total λ(N) index above.

The evolution of δ(N,C), δ(N,H), and δ(C,H) along the IRP is depicted in Figure 1. Mixing of the σ and π densities leads initially to a slight decrease in δ(N,C), at the same time that δ(N,H) and δ(C,H) increase. This trend changes approximately

at the point $R_x = -1$. Then, a sharp electronic reorganization begins. The main changes in electron pairing that are required to evolve from the |C≡N-H to the H-C≡N| structure take place in a relatively small region of the IRP centered around the TS. In fact, the position of the TS in the IRP coincides with the crossing of the δ(N,H) and δ(C,H) curves. However, the catastrophe point which, according to the AIM theory, indicates the change in molecular connectivity from C−N−H to H−C−N, is located clearly before the TS.[6] Actually, such a catastrophe point corresponds to a structure with an HNC angle between 66° and 62°, at about $R_x = -0.75$, a point in the IRP where the electron-pair reorganization is still relatively small with respect to CNH. Remarkably, the system does not have a ring critical point in any point of the IRP.

Another point of interest is the comparison of λ and δ indices in the reactant, TS, and product, in order to determine if the reaction follows the Hammond postulate, from the point of view of the electron-pair distribution. Indeed, most of the λ and δ values in Table 1 reveal that the TS is closer to CNH than to HCN. The same result was reported by Rao from the value of the C−N bond order.[21] A recent study found that, from a structural point of view, this reaction also presents Hammond behavior, with the TS being closer to CNH than to the more stable HCN.[24]

Finally, calculations at the CISD level of theory are used to analyze the effect of Coulomb correlation on the electron pairing for this reaction. Previous studies have shown that, even though the HF method is accurate enough to provide a qualitatively correct picture of the electron pairing taking place in many molecules, consideration of Coulomb correlation generally leads to an increased localization of the electrons in each basin, and a subsequent decrease of the δ indices. These trends are confirmed for CNH, the TS structure, and HCN: in all cases, δ(N,C) decreases considerably when going from the HF to the CISD level, especially for HCN, where there is a difference of ca. 0.4 electrons between the HF (2.24) and the CISD (1.82) values. Delocalization indices between the H atom and the neighboring atom also decrease upon consideration of Coulomb correlation. In general, interatomic distances also increase slightly at the CISD level of theory, in agreement with the decrease in interatomic delocalization. However, delocalization indices between nonbonded atoms, that is, δ(C,H) for CNH and δ(N,H) for HCN, show a slight increase at the CISD level, in spite of having larger interatomic distances. Finally, we have to mention the close similarity between our CISD-optimized geometry of the TS, with H−C and H−N distances and HCN angle of 1.18 Å, 1.41 Å, and 73.1°, respectively (see Scheme 1), and the values obtained by Rao et al.[21] of 1.18 Å, 1.39 Å, and 71.9°, respectively, at the QCISD/TZ2P(d,f) level of theory.

B. $H_2SO \rightarrow$ HSOH Intramolecular Rearrangement. This reaction consists of the transfer of a H from S to O through a TS state in which the H being transferred (H_2) forms a ring with the S and O atoms (see Scheme 1). Thus, in many aspects, this reaction is similar to the CNH to HCN rearrangement discussed above. For instance, the different energy levels of the AO's in the S and O atoms and their effects on the polarities of the SH and OH bonds account for most of the electronic differences between reactant and product for this reaction. Note also that, while the H_2SO molecule has C_{2v} symmetry, no symmetry elements are found for the HSOH system, the TS, and the rest of structures along the IRP. Thus, no analysis in terms of symmetry contributions is performed in this case.

According to the Lewis model, two different structures can be drawn for H_2SO, one predicting a single S−O bond and

TABLE 2: Atomic Populations (N), Localization (λ), and Delocalization (δ) Indices for the Reactant, Transition State, and Product of the $H_2SO \rightarrow$ HSOH Intramolecular Rearrangement Reaction, Calculated at the HF/6-31G* and CISD/6-31G* Levels of Theory

	reactant	TS	product
	(a) HF/6-31G *		
N(S)	15.020	15.514	15.369
$N(H_1)$	0.884	0.994	1.010
$N(H_2)$	0.884	0.583	0.390
λ(O)	8.433	8.081	8.356
λ(S)	13.410	14.005	14.309
$\lambda(H_1)$	0.354	0.445	0.458
$\lambda(H_2)$	0.354	0.144	0.070
$\delta(O,H_1)$	0.089	0.071	0.068
$\delta(O,H_2)$	0.089	0.232	0.617
$\delta(S,H_1)$	0.920	1.015	1.036
$\delta(S,H_2)$	0.920	0.638	0.022
$\delta(H_1,H_2)$	0.052	0.012	0.001
	(b) CISD/6-31G*		
N(O)	9.112	8.890	9.115
N(S)	15.130	15.494	15.482
$N(H_1)$	0.879	0.976	0.982
$N(H_2)$	0.879	0.640	0.420
λ(O)	8.413	8.180	8.312
λ(S)	13.713	14.213	14.534
$\lambda(H_1)$	0.406	0.492	0.496
$\lambda(H_2)$	0.406	0.216	0.107
δ(O,S)	1.226	1.111	0.959
$\delta(O,H_1)$	0.086	0.078	0.066
$\delta(O,H_2)$	0.086	0.232	0.582
$\delta(S,H_1)$	0.804	0.868	0.900
$\delta(S,H_2)$	0.804	0.594	0.039
$\delta(H_1,H_2)$	0.055	0.022	0.007

formal charges of +1 and −1 for S and O, respectively, and a second one with a double S−O bond, and 10 valence electrons on the hypervalent S atom. In contrast, for HSOH, the Lewis model predicts a single S−O bond and no formal charges for the S and O atoms. The HF results (Table 2a) reveal that, for these two molecules, some of the predictions obtained by means of the Lewis model are confirmed within the AIM theory, at least in a qualitative sense. First of all, H_2SO presents charges of +0.98 and −1.21 for the S and O atoms, respectively, which are qualitatively in agreement with the formal charges in the first of the two Lewis structures possible for this molecule. Moreover, S and O present λ values of 13.41 and 8.43, respectively, which reveal that the electron population is sligthly more localized in O (91.6%) than in S (89.3%). Moreover, the value of 1.38 for δ(O,S) reveals some double bond character for the S−O bond, which can be related to the contribution of the second Lewis structure. In fact, the δ(O,S) value is far from 2 because of the different electronegativities of the atoms involved. For the HSOH molecule, the Lewis model predicts no formal charges; however, the AIM charges for S and O are −1.23 and +0.63, respectively. This is just a consequence of the fact that the Lewis model does not consider the different electronegativities of the S and O atoms. With respect to the reactant molecule, λ(O) decreases (8.36), in spite of the O atom having the same population in both molecules, while λ(S) increases (14.31). Thus, in this case, the electron population of S is more localized (93.1%) than that of O (90.5%). The δ(O,S) value of 1.06 is consistent with a covalent single bond between S and O; however, the fact that δ(O,S) is slightly larger than 1, in spite of the different electronegativities of these atoms, might be indicative of some double-bonding character between S and O.

The H atoms also change significantly between reactants and products. First of all, in H_2SO, both H atoms are equivalent.

λ(H) and δ(S,H) values are 0.35 and 0.92, respectively, revealing that the S−H bond is covalent but polarized toward S. The atomic charges in the H atoms (+0.12) also show a slight transfer of charge from the H's to the SO group. However, the situation is quite different for HSOH. Here, the two H's are no longer equivalent, and the localization and delocalization indices show significant differences between the S−H_1 and O−H_2 bonds. On the one hand, the values of N(H_1) (1.01), λ(H_1) (0.46), and δ(S,H_1) (1.04) associated to the SH fragment correspond to a nearly perfect covalent bond. On the other hand, the OH bond appears to be very polar. For instance, the atomic population on H_2 is only 0.39 (a charge of +0.61), and λ(H_2) is also very small (0.07), while δ(O,H_2) is 0.62. Finally, it is worth remarking that delocalization indices between nonbonded atoms always have small values; however, for H_2SO, the δ indices between nonbonded atoms sum up to a total of 0.23 electrons.

The TS structure presents λ and δ values that are intermediate between those of reactants and products. The most significant ones are the delocalization indices between the H being transferred and the heavy atoms: 0.64 and 0.23 for δ(S,H_2) and δ(O,H_2), respectively, which show that, at the TS, the charge density associated to H_2 is delocalized between the three atoms directly involved in the reaction. Note that the values of δ(S,H_2) and δ(O,H_2) in the TS are closer to the values in the reactant than in the product (see Table 2). The same trend is found also for δ(O,S) which is 1.38, 1.37, and 1.06 for the reactant, TS, and product, respectively. The λ(H_1), λ(H_2), and λ(S) at the TS are also intermediate between those in H_2SO and HSOH. However, in these cases, the values at the TS are closer to the product than to the reactant. Finally, λ(O) is minimal at the TS. Interestingly, N(O) is also minimal at the TS, while N(S) is maximal. Thus, at the TS, the charge transfer from S to O is minimal.

The λ and δ values discussed above, especially δ(S,H_2), δ(O,H_2), and δ(O,S), seem to indicate that the TS is closer to H_2SO than to HSOH, from the point of view of the electron-pair distribution. At this point, it is interesting to recall that previous studies,[23,24] using a measure of structural proximity based on similarities between one-electron densities, found an anti-Hammond behavior for this reaction, with the TS being structurally closer to the more stable HSOH. Moreover, the geometrical parameters of the three structures discussed confirm that, from a geometrical point of view, the TS is also more similar to HSOH than to H_2SO (see Scheme 1). For instance, the S−O distance, the S−H_2 distance, and the HSOH dihedral angle in the TS and in HSOH are very similar. Thus, according to these results, the evolution from H_2SO to the TS implies a significant geometrical rearrangement, including an increase of 0.16 Å in the S−O distance and ca. 90° in the dihedral angle, while the geometrical reorganization needed to go from the TS to HSOH is much smaller. In contrast, the changes in electron pairing are more important when going from TS to product than from reactant to TS.

More insight on the electron-pair processes taking place along the reaction can be obtained by following the evolution of the delocalization indices along the reaction path (Figure 2). Three different topological structures are found along the IRP. First, for all structures between the reactant and TS, analysis of the electron density yields three bond critical points, associated to two H−S and one S−O bonds. In contrast, the first point after the TS (R_x = 0.20) shows a ring structure between S, O, and H_2, with H_1 attached to S. Finally, from the next point (R_x = 0.40) to the end of the IRP, the molecular graph corresponds to H−S−O−H. Figure 2 shows that both the changes in the topology of the electron density and in the electron pairing patterns are restricted to a small region of the IRP around the TS (between $R_x = -1$ and $R_x = +1$). Within this region, there is a sudden decrease of δ(S,H_2) at the same time that δ(O,H_2) increases, corresponding to the transfer of H_2 from S to O. This transfer has also a small effect on the delocalization between S and H_1. Thus, δ(S,H_1) increases slightly when going from reactants to products. Finally, there are also significant changes in δ(O,S) during the rearrangement process. First of all, δ(O,S) increases slightly when going from the reactant to the TS, where it reaches a maximum value. Then, δ(O,S) decreases again to reach a value of 1.06 at the product molecule.

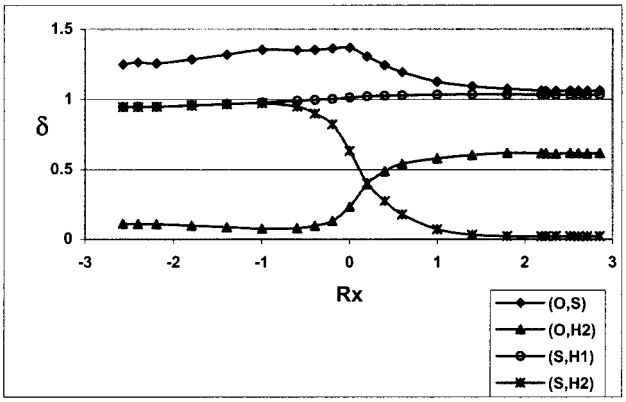

Figure 2. Evolution of the values of selected delocalization indices along the $H_2SO \rightarrow$ HSOH rearrangment reaction, calculated at the HF/6-31G* level of theory. Negative and positive values of the reaction coordinate (R_x) correspond to reactant (H_2SO) and product (HSOH), respectively. The TS is located at $R_x = 0$.

Finally, comparison of HF and CISD results (see Table 2b) shows that, in general, Coulomb correlation reduces the charge transfer between atoms, increases the atomic localization, decreases the delocalization between bonded atoms, and increases slightly the delocalization between nonbonded atoms. Moreover, CISD also increases slightly the interatomic distances (see Scheme 1). In general, the HF−CISD differences on λ and δ indices are not larger than 0.1 electrons, except for δ(O,S), where the differences are ca. 0.15, 0.25, and 0.10 electrons for the reactant, TS, and product, respectively. Thus, at the CISD level, regarding the δ(O,S) value, the differences between H_2SO and the TS become larger, while the differences between the TS and HSOH become smaller, compared to the HF results. In summary, from an electron-pairing perspective, CISD moves the structure of the TS toward the reactant. However, the main conclusions of the analysis of the reaction at the HF level are also valid at the CISD level of theory.

C. $CH_3Cl + F^- \rightarrow Cl^- + CH_3F$ Nucleophilic Substitution. This reaction consists of the S_N2 nucleophilic substitution of the Cl atom in CH_3Cl by a F atom. Reactant and product molecules correspond to the [$ClCH_3\cdots F^-$] and [$Cl^-\cdots CH_3F$] complexes, respectively, while the TS corresponds to a [$Cl\cdots CH_3\cdots F]^-$ structure (see Scheme 1). The reaction proceeds through a progressive lengthening of the C−Cl distance, at the same time that the C−F distance decreases and there is an inversion of the umbrella in the CH_3 group. The [$Cl\cdots CH_3\cdots F]^-$ TS structure corresponds to a point where the Cl−C and C−F distances are very similar (2.13 and 2.12 Å, respectively) and the CH_3 group is slightly bend in the direction of the smaller F atom (the H−C−Cl angle is ca. 97°). In the reactant complex (RC), the distance between C and F is 2.6 Å, while the C−Cl distance in the product complex (PC) is 3.4 Å. Finally, even though the C_{3v} symmetry is preserved along all the reaction

TABLE 3: Atomic Populations (N), Localization (λ), and Delocalization (δ) Indices for the Reactant, Transition State, and Product of the $CH_3Cl + F^- \rightarrow Cl^- + CH_3F$ Nucleophilic Substitution Reaction, Calculated at the HF/6-31G* Level of Theory

	reactant	TS	product
N(Cl)	17.491	17.681	17.980
N(C)	5.799	5.745	5.374
N(H)	0.910	0.882	0.962
N(F)	9.981	9.926	9.760
λ(Cl)	16.939	17.274	17.922
λ(C)	3.904	3.928	3.603
λ(H)	0.375	0.354	0.424
λ(F)	9.894	9.740	9.304
δ(Cl,C)	0.910	0.626	0.042
δ(Cl,H)	0.059	0.050	0.023
δ(C,H)	0.934	0.927	0.929
δ(C,F)	0.080	0.229	0.714
δ(H,H)	0.026	0.023	0.030
δ(H,F)	0.027	0.035	0.064

paths, the contributions of electrons belonging to different symmetry species cannot be separated in this case.

According to the HF results (Table 3), both the $[ClCH_3\cdots F^-]$ and $[Cl^-\cdots CH_3F]$ complexes present an anion, F^- or Cl^-, forming a long distance closed-shell interaction with the CH_3-Cl or CH_3F molecule, respectively. Thus, both the F atom in $[ClCH_3\cdots F^-]$ and the Cl atom in $[Cl^-\cdots CH_3F]$ have atomic charges of -0.98 electrons. Moreover, comparison of the atomic populations to the corresponding λ(F) and λ(Cl) indices reveal that more than 99% of the electronic population in each of the anions is localized in its own atomic basin. Delocalization indices between the anion and the C atom are small in both the RC (0.08) and the PC (0.04).

According to the λ and δ indices for the CH_3Cl and CH_3F moieties within the RC and PC, both molecules present three covalent C−H bonds, plus a polar C−Cl or C−F bond. λ and δ indices confirm that the C−Cl bond in CH_3Cl is less polar than the C−F bond in CH_3F. Thus, for the RC, atomic charges are $+0.20$ and -0.49 on C and Cl, respectively, while δ(C,Cl) is 0.91. Furthermore, the PC shows a larger degree of charge transfer between C ($+0.63$) and F (-0.76), and a smaller electron delocalization between these atoms (δ(Cl,C) = 0.71). In contrast, the H atoms are found to be very similar in the reactant and product complexes. For instance, in both cases, the H atoms present small positive charges (less than $+0.1$), λ(H) values of ca. 0.4 and δ(C,H) values of 0.93. Finally, it is worth pointing out that, in both complexes, there is some degree of electron delocalization between the H atoms themselves and between each of the H atoms and the F and Cl atoms. Even though the δ values corresponding to these kind of interactions are quite small (between 0.02 and 0.06), there is a total of ca. 0.35 electrons delocalized between nonbonded atoms in both complexes.

Once the electronic structure of the RC and PC has been discussed, we proceed to analyze the $[Cl\cdots CH_3\cdots F]^-$ complex corresponding to the TS. First of all, δ(C,H) has approximately the same value (0.93) as in the RC and PC, revealing that the sharing of the electron pairs between C and each of the H atoms is preserved along the reaction. However, both N(H) (0.88) and λ(H) (0.35) are minimal at the TS with respect to the RC and PC. As for the C atom, even though N(C) at the TS (5.75) is intermediate between the N(C) values at the reactant and product complexes, λ(C) is maximal at the TS (3.93); thus, the percentage of electron localization at the C atom is maximal at the TS, which can be attributed to the fact that both C−F and C−Cl interactions are weak at the TS. N and λ values for the rest of atoms are always intermediate between the values at the RC and PC. In particular, δ(Cl,C) and δ(C,F) are 0.63 and 0.23 at the TS, respectively, revealing that the TS is electronically closer to the RC. Interestingly, despite the similarity between the C−Cl and C−F distances at the TS, δ(Cl,C) is larger than δ(C,F), which can be attributted to the diffuse nature of the valence orbitals in Cl. Moreover, the H−C−Cl angle (97°) denotes that, at the TS, the CH_3 umbrella is still pointing toward the F atom. All in all, these data reveal that, in terms of both geometry and electron-pair structure, the TS is closer to the RC than to the PC.

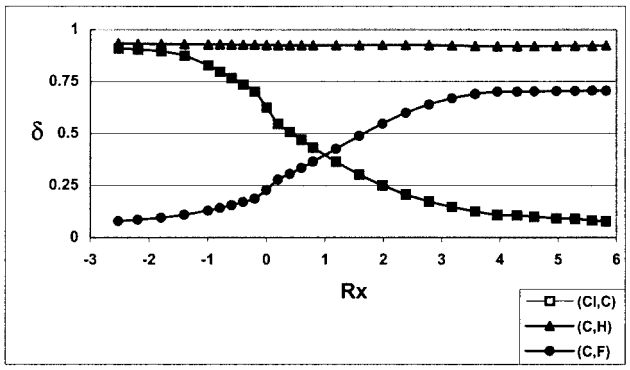

Figure 3. Evolution of the values of selected delocalization indices along the $FCH_3 + Cl^- \rightarrow F^- + CH_3Cl$ S_N2 reaction, calculated at the HF/6-31++G* level of theory. Negative and positive values of the reaction coordinate (R_x) correspond to reactant ($[FCH_3\cdots Cl]^-$) and product ($[F\cdots CH_3Cl]^-$) complexes, respectively. The TS is located at $R_x = 0$.

Figure 3 shows the evolution of selected delocalization indices along the reaction path, confirming that δ(Cl,C) and δ(C,F) account for most part of the electron-pair reorganization taking place during the reaction. Moreover, it is also made evident that the TS occurs early in the reaction path and close to the RC. Indeed, the point in the IRP where the values of δ(Cl,C) and δ(C,F) are approximately the average of the corresponding values at the RC and PC is found after the TS (R_x ca. $+0.40$), while the crossing between δ(Cl,C) and δ(C,F) takes place later (R_x ca. $+1.00$). Furthermore, this graph shows also that, in contrast to the rearrangement reactions discussed above, the electron-pair reorganization in this S_N2 reaction takes place gradually along the reaction path; that is, there is a large region in the IRP where there is significant Cl−C and F−C delocalization at the same time. Moreover, the molecular connectivity is preserved along the reaction, and no catastrophe points are found.

D. $HF + C_2H_4 \rightarrow C_2H_5F$ Electrophilic Addition. For this reaction, the RC consists of a HF molecule with the H atom pointing toward the double bond in C_2H_4, with the H atom in HF (H_5) located at approximately 2.5 Å from the two C atoms in C_2H_4. The HF molecule is located in the symmetry plane bisecting the C_2H_4 molecule, with the F atom deviating slightly from the perpendicular to the C−C bond. The reaction proceeds through a TS state with the two C atoms, F, and H_5 forming a ring. The product corresponds to the C_2H_5F molecule in a staggered conformation (see Scheme 1).

At the Hartree−Fock level of theory, atomic populations, and localization and delocalization indices for the HF molecule in the RC show that the electron pair shared between H_5 and F is heavily polarized toward F. Thus, there is a transfer of ca. 0.7 electrons from H_5 to F, and $\lambda(H_5)$ is very small (0.03). However, there is a still nearly half an electron (0.44) delocalized between F and H_5 (see Table 4a). As for the C_2H_4 molecule, there is

TABLE 4: Atomic Populations (N), Localization (λ), and Delocalization (δ) Indices for the Reactant, Transition State, and Product of the HF + $C_2H_4 \rightarrow C_2H_5F$ Electrophilic Addition Reaction, Calculated at the HF/6-31G* and CISD/6-31G* Levels of Theory

	reactant	TS	product
	(a) HF/6-31G *		
$N(C_2)$	6.051	5.887	5.305
$N(H_3)$	0.967	0.967	1.012
$N(H_5)$	0.277	0.453	1.002
$N(F_6)$	9.754	9.791	9.747
$N(H_7)$	0.964	0.890	1.003
$\lambda(C_1)$	4.061	4.198	3.922
$\lambda(C_2)$	4.053	4.017	3.482
$\lambda(H_3)$	0.428	0.422	0.464
$\lambda(H_5)$	0.032	0.085	0.455
$\lambda(F_6)$	9.511	9.379	9.262
$\lambda(H_7)$	0.425	0.370	0.466
$\delta(C_1,C_2)$	1.893	1.338	0.972
$\delta(C_1,H_3)$	0.970	0.970	0.965
$\delta(C_1,H_5)$	0.023	0.382	0.962
$\delta(C_2,H_5)$	0.027	0.090	0.039
$\delta(C_2,F_6)$	0.027	0.323	0.717
$\delta(C_2,H_7)$	0.968	0.936	0.918
$\delta(H_5,F_6)$	0.435	0.243	0.008
	(b) CISD/6-31G*		
$N(C_1)$	6.107	6.248	6.023
$N(C_2)$	6.107	5.905	5.414
$N(H_3)$	0.937	0.944	0.982
$N(H_5)$	0.310	0.472	0.972
$N(F_6)$	9.728	9.725	9.692
$N(H_7)$	0.937	0.883	0.974
$\lambda(C_2)$	4.474	4.313	3.845
$\lambda(H_3)$	0.451	0.451	0.488
$\lambda(H_5)$	0.054	0.113	0.480
$\lambda(F_6)$	9.480	9.293	9.224
$\lambda(H_7)$	0.451	0.410	0.490
$\delta(C_1,C_2)$	1.474	1.100	0.821
$\delta(C_1,H_3)$	0.834	0.837	0.815
$\delta(C_1,H_5)$	0.034	0.345	0.813
$\delta(C_2,H_5)$	0.034	0.072	0.034
$\delta(C_2,F_6)$	0.033	0.333	0.667
$\delta(C_2,H_7)$	0.834	0.793	0.773
$\delta(H_5,F_6)$	0.441	0.268	0.019

significant electron delocalization between each C atom and its neighbor H's (0.97), as well as between the two C atoms (1.89). Moreover, all the atomic charges are very small, and the localization indices are ca. 4.05 and 0.43 for the C and H atoms, respectively. Altogether, these data reveal that each C atom is sharing an electron pair with each of its bonded H's, and the two C atoms are sharing two pairs of electrons. In all these cases, the electrons are shared equally between each pair of bonded atoms. Finally, delocalization indices between atoms in the C_2H_4 and HF molecules are very small, revealing that the interaction between the two molecules in the complex is weak.

Table 4a also gathers the results for the CH_3CH_2F molecule resulting from the addition reaction. The N and λ values for the C atoms reflect that, compared to C_2H_4, the C atoms in CH_3-CH_2F have lower atomic populations and localization indices, especially the C atom bonded to F. In contrast, with respect to the HF molecule, the F atom has nearly the same atomic population (ca. 9.7), but has a lower localization index (9.26 in front of 9.51). Accordingly, $\delta(C_2,F_6)$ in CH_3CH_2F is much larger (0.72) than $\delta(H_5,F_6)$ in HF (0.44), in agreement with the different polarities of the F−H and F−C bonds compared. Although there are three classes of nonequivalent H's in CH_3CH_2F, all of them present similar characteristics, that is, atomic populations of ca. 1.0 and localization indices of 0.46. All the H's in the CH_3 group present a delocalization index of 0.96 with the C atoms,

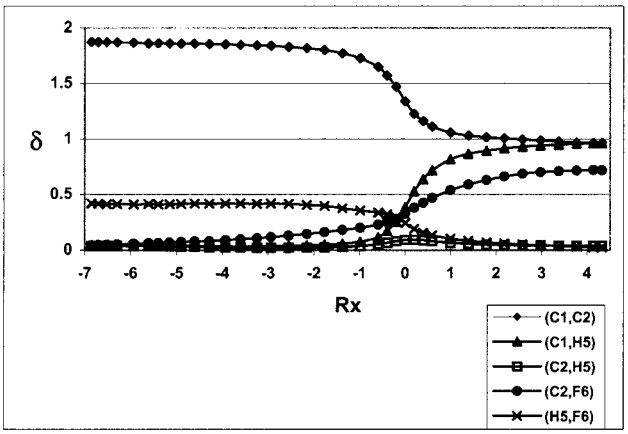

Figure 4. Evolution of the values of selected localization and delocalization indices along the C_2H_4 + HF $\rightarrow$ C_2H_5F reaction, calculated at the HF/6-31G* level of theory. Negative and positive values of the reaction coordinate (R_x) correspond to reactant complex ($C_2H_4\cdots$HF) and product (C_2H_5F), respectively. The TS is located at $R_x = 0$.

while the two H atoms in the CH_2F group have a lower δ(C,H) value (0.92).

In general, the electron-pairing pattern in the TS structure is intermediate between the RC and the product. This is especially true for most of delocalization indices undergoing major changes during the reaction, that is, $\delta(C_1,C_2)$, $\delta(C_1,H_5)$, $\delta(C_2,F_6)$, and $\delta(H_5,F_6)$. The $\delta(C_1,C_2)$ value in the TS (1.34) is closer to that in the product than in the reactant; however, this trend is not shared by the rest of δ indices mentioned above. Therefore, according to these indices, one cannot decide clearly whether the TS is closer to the RC or the product, from an electronic point of view. Furthermore, some of the N and λ values in the TS are not intermediate between those in the RC and the product. $N(C_1)$, $N(F_6)$, and $\lambda(C_1)$ are maximal at the TS, while $\lambda(H_3)$ and $\lambda(H_7)$ are minimal. Interestingly, $\delta(C_2,H_5)$ is also maximal at the TS (0.09).

Figure 4 shows the evolution of some significant delocalization indices along the IRP. For a large region of the IRP ($R_x < -1$), which corresponds to HF approaching C_2H_4, the δ indices change slowly. Then, in a small region around the TS ($-1 < R_x < +1$), the $\delta(C_1,C_2)$, $\delta(C_1,H_5)$, $\delta(C_2,F_6)$, and $\delta(H_5,F_6)$ indices suffer a rapid evolution. Furthermore, $\delta(C_2,H_5)$, which has negligible values all along the IRP, increases slightly in this region. This corresponds to the process of maximal electron-pair reorganization, where H_5 is transferred from F to C_1, through a TS in which H_5 is located relatively near to C_2. Finally, the last part of the IRP basically corresponds to the geometrical reorganization needed for the C_2H_5F molecule to reach the final staggered conformation. The topology of the electron density is not constant throughout the reaction. For the RC, the interaction between the two molecules takes place through a C_2–H_5 bond, while in the TS the two C atoms and the HF molecule form a ring, while there are no rings in the product molecule. Other topologies are found between the RC and the TS; indeed, there are five catastrophe points during the reaction.

Table 4b gathers the CISD results for this reaction, which are qualitatively equivalent to the Hartree−Fock ones. The main effects of including Coulomb correlation, with respect to the HF reference, are those already found in other cases; in general, CISD yields larger interatomic distances, reduces the charge transfer between atoms, increases the atomic localization, and reduces the electronic delocalization between pairs of bonded

TABLE 5: Atomic Populations (N), Localization (λ), and Delocalization (δ) Indices for the Reactants, Transition State, and Product of the $C_2H_4 + C_4H_6 \rightarrow C_6H_{10}$ Diels−Alder Cycloaddition Reaction, Calculated at the HF/6-31G* Level of Theory

	reactants			
	butadiene	ethylene	TS	product
$N(C_1)$	6.010		5.992	6.056
$N(C_5)$		6.035	6.030	5.911
$N(C_6)$	6.033		6.039	5.909
$N(H_9)$	0.979		0.988	1.027
$N(H_{12})$		0.983	0.981	1.036
$N(H_{13})$		0.983	0.990	1.035
$N(H_{14})$	0.985		0.981	1.027
$N(H_{15})$	0.994		1.000	1.001
$\lambda(C_1)$	3.960		3.928	3.998
$\lambda(C_5)$		4.042	3.976	3.846
$\lambda(C_6)$	4.037		3.990	3.846
$\lambda(H_9)$	0.437		0.442	0.475
$\lambda(H_{12})$		0.441	0.431	0.481
$\lambda(H_{13})$		0.441	0.439	0.483
$\lambda(H_{14})$	0.438		0.424	0.473
$\lambda(H_{15})$	0.450		0.454	0.455
$\delta(C_1,C_2)$ o	1.068		1.347	1.828
$\delta(C_1,C_6)$ o	1.839		1.438	1.008
$\delta(C_4,C_5)$ o		1.924	1.455	0.978
$\delta(C_5,C_6)$ o			0.397	0.976
$\delta(C_1,H_{15})$	0.959		0.961	0.963
$\delta(C_5,H_{12})$		0.972	0.960	0.945
$\delta(C_5,H_{13})$		0.972	0.959	0.951
$\delta(C_6,H_9)$	0.972		0.967	0.946
$\delta(C_6,H_{14})$	0.965		0.942	0.941
$\delta(C_1,C_3)$ m	0.067		0.073	0.043
$\delta(C_1,C_4)$ p			0.086	0.009
$\delta(C_1,C_5)$ m			0.050	0.059
$\delta(C_3,C_6)$ p	0.072		0.103	0.014
$\delta(C_4,C_6)$ m			0.042	0.059

[a] o, m, and p are used to denote pairs of atoms that are in ortho, meta and para, respectively, in the TS.

atoms. Moreover, at the CISD level, the HF molecule in the RC is exactly perpendicular to the C−C bond.

E. $C_2H_4 + C_4H_6 \rightarrow C_6H_{10}$ Diels−Alder Cycloaddition. The Diels−Alder reaction between butadiene and ethylene to yield hexadiene is often taken as the prototype of a pericyclic concerted reaction (see Scheme 1 for a description of the RC, TS, and product involved in this reaction).

Table 5 gathers atomic populations and localization indices for all nonequivalent atoms of the reactants, TS, and product for the concerted Diels−Alder reaction, calculated at the HF level of theory. Delocalization indices are reported only for relevant nonequivalent pairs of atoms. First of all, the atomic populations reveal that the charge transfer between atoms is virtually inexistent in the three structures. Thus, populations for all the C and H atoms are always ca. 6.0 and 1.0, respectively. Moreover, λ indices range between 0.4 and 0.5 for the H atoms, and between 3.8 and 4.0 for the C atoms. Indeed, the major changes along the reaction involve a slight decrease of ca. 0.2 e in $\lambda(C_5)$ and $\lambda(C_6)$, which correspond to the C atoms involved in the formation of new bonds, and an increase of 0.07 e in $\lambda(C_1)$. Interestingly, slightly different λ(C) and λ(H) values are obtained for aliphatic and olefinic atoms. For instance, in the hexadiene molecule, λ(C) is 3.85 for the aliphatic C_5 and C_6 atoms, and 4.00 for the olefinic C_1 atom. The reverse trend is found for the hydrogen atoms: λ(H) takes values of 0.48 for the H_{12} and H_{13} atoms, respectively, and 0.47 for the H_9 and H_{14} atoms, respectively, while it is 0.45 for the olefinic H_{15} atom.

The δ(C,H) indices have values between 0.9 and 1.0, corresponding to a rather apolar sharing of the electrons between the C and H atoms, and also remain nearly constant throughout the reaction. Indeed, the most significant changes during the Diels−Alder reaction are found in the δ(C,C) indices. For the three structures, pairs of C atoms that are formally single-bonded present values of δ(C,C) between 1.0 and 1.1, while formally double-bonded C atoms correspond to δ(C,C) values between 1.8 and 1.9. For the reactants, it is interesting to remark that δ(C,C) values between double-bonded atoms are lower for butadiene (1.83) than for ethene (1.92), while δ(C,C) values between single-bonded atoms in butadiene are slightly larger than 1 (1.07), revealing, as expected, that the C−C bonds in butadiene have intermediate character between a single and a double typical bond. Moreover, delocalization indices between nonbonded C's in butadiene reveal that 1,4 delocalization ($\delta(C_3,C_6) = 0.072$) is slightly more important than 1,3 delocalization ($\delta(C_3,C_6) = 0.067$). δ(C,C) values for reactants and products are consistent with the formation of a new bond between the C_5 and C_6 atoms (and the equivalent C_4 and C_3 atoms). At the same time, the C_1–C_2 single bond of the butadiene molecule evolves to a double bond in the hexadiene molecule, while the C_4–C_5 double bond in ethene and the C_1–C_6 and C_2–C_3 double bonds in butadiene are transformed to formal single bonds in hexadiene.

The TS in this reaction corresponds to a nonplanar structure with the six carbon atoms forming a ring. This structure is usually considered to be aromatic, and theoretical calculations of magnetic susceptibilities and ^{1}H chemical shifts support this point of view.[30] Indeed, according to the localization and delocalization indices reported in Table 5, the TS is clearly aromatic. First of all, one must take into account that there are three nonequivalent C atoms (e.g., C_1, C_5, and C_6). Therefore, there exist the following pairs of nonequivalent C pairs: four ortho pairs, three meta pairs, and two para pairs (see Scheme 1). For the ortho pairs, the associated δ(C,C) indices are ca. 1.4, except for $\delta(C_5,C_6)$, and the equivalent $\delta(C_3,C_4)$, which are ca. 0.40. Therefore, from an electronic point of view, this structure is nearly equivalent to that of the benzene molecule, with the difference that there is no σ bonding associated to the C_3–C_4 and C_5–C_6 pairs. Moreover, values for δ(C,C) indices associated to pairs of C atoms in meta are rather small (ranging from 0.04 to 0.07), while pairs of atoms in para present slightly larger δ(C,C) values (0.09 and 0.10). The fact that there is more delocalization between atoms in para than between atoms in meta, in spite of the larger interatomic distance between atoms in para, is characteristic of aromatic systems.[37] Thus, according to the δ(C,C) values discussed above, one can consider that the TS presents a set of six π electrons delocalized between the six C atoms, although the nonplanar character of this structure prevents from separating strictly the electrons into σ and π sets. Furthermore, the fact that different C−C distances exist (ca. 1.4 Å for the σ bonded atom pairs, and ca. 2.2 Å for the C_3–C_4 and C_5–C_6 pairs) leads to slightly different delocalizations for the different ortho, meta, and ortho pairs; however, it is remarkable that the main electron delocalization patterns associated to aromaticity take place in spite of the large C_3–C_4 and C_5–C_6 distances. A comparison of the different ortho δ(C,C) values reveals that the electron delocalization is slightly larger between the C_1–C_6 , C_4–C_5, and C_2–C_3 pairs. Hence, from an electronic point of view, the TS is closer to the reactant than to the product. Moreover, an analysis of the C−C distances in the reactants, TS, and product reveals that this reaction does also follow the Hammond principle from a structural point of view.

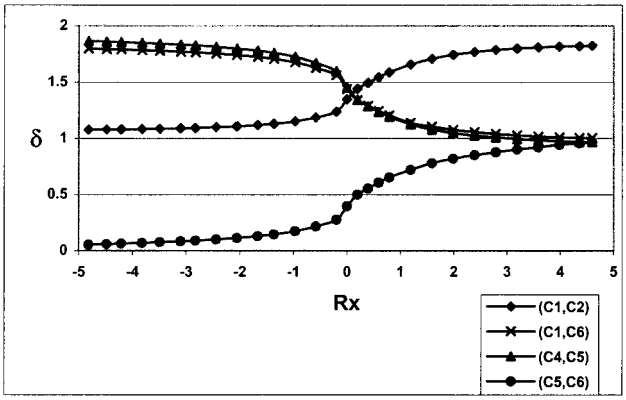

Figure 5. Evolution of the values of selected delocalization indices along the Diels−Alder cycloaddition reaction, calculated at the HF/6-31G* level of theory. Negative and positive values of the reaction coordinate (R_x) correspond to reactants ($C_2H_4 + C_4H_6$) and product (C_6H_{10}), respectively. The TS is located at $R_x = 0$.

Finally, the evolution of the C_1–C_2, C_1–C_6 , C_4–C_5, and C_5–C_6 delocalization indices along the IRP is depicted in Figure 5. This graph reflects clearly the evolution of the electron-pair patterns associated to this cycloaddition reaction. Although all the electron delocalization indices vary gradually along the IRP, the main changes in electron-pair reorganization take place mainly in a small region around the TS.

Conclusions

Electronic localization and delocalization indices, calculated according to the AIM theory, have been used to study the electron-pair reorganization taking place in five different chemical reactions. For most of the molecular structures described, the electron-pair picture provided by λ and δ indices is qualitatively in good agreement with the predictions made by means of the Lewis model, especially at the HF level of theory. λ and δ indices describe accurately subtle electronic differences between molecular structures that are electronically equivalent in the simple Lewis model, and reflect the gradual electronic changes taking place along a reaction path. In this respect, it is remarkable that, for some reactions studied, the main changes in charge density topology and in electron pairing take place at different points of the IRP. Thus, λ and δ indices provide useful information that cannot be obtained from a simple charge density analysis. Finally, delocalization indices in the TS state of the concerted Diels−Alder reaction are able to detect the aromaticity of this structure and reveal that there is not a simple correlation between interatomic distance and electron delocalization.

An important feature of the analysis proposed in this paper is that it is model independent, λ and δ indices being obtained only from first- and second-order densities, which are physical observables. In principle, there is no need to resort to any particular model, such as MO theory for these calculations. Therefore, provided that $\rho^{\sigma}(\mathrm{r})$ and $\Gamma^{\sigma\sigma'}(\mathbf{r}_1,\mathbf{r}_2)$ are available, this analysis could be performed at any level of theory. At present, practice provides second-order densities only for the HF and CISD approximations.

The comparison of the results obtained at the two levels of theory confirm that, for reactions correctly described at the HF level, both methods yield qualitatively similar results. However, the neglect of Coulomb correlation within the HF approximation leads to interatomic delocalization values that are generally too large.

In summary, λ and δ indices, together with AIM atomic populations, have been found very useful for describing accurately the changes in electron pairing that takes place along the reaction path for a number of reactions in the gas phase.

Acknowledgment. This work was supported by the Spanish DGES Project No. PB98-0457-C02-01. J.P. benefited from the doctoral fellowship no. 2000FI-00582 from the Generalitat de Catalunya.

References and Notes

(1) Lewis G. N. *J. Am. Chem. Soc.* **1916**, *38*, 762.
(2) McWeeny, R. *Rev. Mod. Phys.* **1960**, *32*, 335.
(3) Cooper, I. L.; Pounder C. N. M. *Theor. Chim. Acta* **1973**, *47*, 51. Doggett, G. *Mol. Phys.* **1977**, *34*, 1739. Luken, W. L.; Beratan, D. N. *Theor. Chim. Acta* **1982**, *61*, 265. Luken, W. L. *Croat. Chem. Acta* **1984**, *57*, 1283. Tschinke, V.; Ziegler, T. *J. Chem. Phys.* **1990**, *93*, 8051. Baerends, E. J.; Gritsenko, O. V. *J. Phys. Chem.* **1997**, *101*, 5383.
(4) Bader, R. F. W.; Stephens, M. E. *J. Am. Chem. Soc.* **1975**, *97*, 7391. R. F. W. Bader; Streitwieser, A.; Neuhaus, A.; Laidig, K. E.; Speers, P. *J. Am. Chem. Soc.* **1996**, *118*, 4959. Bader, R. F. W.; Johnson, S.; Tang, T.-H. *J. Phys. Chem.* **1996**, *100*, 15398. Gillespie, R. J.; Bayles, D.; Platts, J.; Heard, G. L.; Bader, R. F. W. *J. Phys. Chem. A* **1996**, *102*, 3407.
(5) Fradera, X.; Duran, M.; Mestres, J. *J. Comput. Chem.* **2000**, *21*, 1361.
(6) Bader, R. F. W. *Atoms in Molecules: A Quantum Theory*; Oxford University Press: Oxford, UK, 1990.
(7) See Ref. 5., and also Ponec, R. *J. Math. Chem.* **1997**, *21*, 323. Ponec, R. *J. Math. Chem.* **1998**, *23*, 85. Ponec, R.; Duben, A. J. *J. Comput. Chem.* **1999**, *20*, 760.
(8) Becke, A. D.; Edgecombe, K. E. *J. Chem. Phys.* **1990**, *92*, 5397. Silvi, B.; Savin, A. *Nature* **1994**, *371*, 683.
(9) Fradera, X.; Austen, M. A.; Bader, R. F. W. *J. Phys. Chem. A* **1999**, *103*, 304.
(10) Bader, R. F. W.; Bayles, D. *J. Phys. Chem. A* **2000**, *104*, 5579.
(11) Wiberg, K. B. *Tetrahedron* **1968**, *24*, 1083.
(12) Ponec, R.; Uhlik, F. *J. Mol. Struct. (THEOCHEM)* **1997**, *391*, 159. Ponec, R.; Carbó-Dorca, R. *Int. J. Quantum Chem.* **1999**, *72*, 85. Bochicchio, R.; Ponec, R.; Lain, L.; Torre, A. *J. Phys. Chem. A* **2000**, *104*, 9130.
(13) Dobado, J. A.; Martínez-García, H.; Molina Molina, J.; Sundberg, M. R. *J. Am. Chem. Soc.* **2000**, *122*, 1144. El-Bergmi, R.; Dobado, J. A.; Portal, D.; Molina Molina, J. *J. Comput. Chem.* **2000**, *21*, 322. Dobado, J. A.; Molina Molina, J.; Uggla, R.; Sundberg, M. R. *Inorg. Chem.* **2000**, *39*, 2831.
(14) Chesnut, D. B.; Bartolotti, L. J. *Chem. Phys.* **2000**, *257*, 175.
(15) Burke, K.; Perdew, J. P.; Ernzerhof, M. *J. Chem. Phys.* **1998**, *109*, 3760. Poater, J.; Solà, M.; Duran, M.; Fradera, X., to be submitted for publication.
(16) Ángyán, I.; Loos. M.; Mayer, I. *J. Phys. Chem.* **1994**, *98*, 5244.
(17) Fulton, R. L. *J. Phys. Chem.* **1993**, *97*, 7516.
(18) Cioslowski, J.; Mixon, S. T. *J. Am. Chem. Soc.* **1991**, *113*, 4142.
(19) Yamasaki, T.; Goddard III, W. A. *J. Phys. Chem. A* **1998**, *102*, 2919. Yamasaki, T.; Mainz, D. T.; Goddard III, W. A. *J. Phys. Chem. A* **2000**, *104*, 2221.
(20) Ponec, R. *Collect. Czech. Chem. Commun.* **1997**, *62*, 1821. Ponec, R. *Int. J. Quantum Chem.* **1997**, *62*, 171. Lendvay, G. *J. Phys. Chem.* **1989**, *93*, 4422. Maity, D. K.; Majumdar, D.; Bhattacharyya, S. P. *J. Mol. Sruct. (THEOCHEM)* **1992**, *276*, 315. Lendvay, G. *J. Phys. Chem.* **1994**, *98*, 6098. Oliva, J. M.; Gerratt, J.; Karadakov, P. B.; Cooper, D. L. *J. Chem. Phys.* **1997**, *107*, 8917.
(21) Rao, S. V. *J. Comput. Chem.* **2000**, *21*, 1283.
(22) Pearson, P. K.; Schaefer, H. F., III. *Chem. Phys.* **1975**, *62*, 350. Müller, K.; Brown, L. D. *Theor. Chim. Acta* **1979**, *53*, 75. Gray, S. K.; Miller, W. H.; Yamaguchi, Y.; Schaefer, H. F., III. *J. Chem. Phys.* **1980**, *73*, 2733. Garret, B. C.; Redmon, M. J.; Steckler, R.; Truhlar, D. G.; Baldridge, K. K.; Bartol, D.; Schmidt, M. W.; Gordon, M. S. *J. Phys. Chem.* **1988**, *92*, 1476. Fan, L. Y.; Ziegler, T. *J. Chem. Phys.* **1990**, *90*, 3645. Bentley, J. A.; Bowman, J. M.; Gazdy, B.; Lee, T. J.; Dateo, C. E. *Chem. Phys. Lett.* **1992**, *198*, 563. Fan, L. Y.; Ziegler, T. *J. Am. Chem. Soc.* **1992**, *114*, 10890. Bentley, J. A.; Huang, C. N.; Wyatt, R. E. *J. Chem. Phys.* **1993**, *98*, 5207. Eriksson, L. A.; Lopez, X.; Boyd, R. J. *J. Phys. Chem.* **1993**, *97*, 11969. Jursic, B. S. *Chem. Phys. Lett.* **1996**, *256*, 213. Mineva, T.; Sicilia, E.; Russo, N. *J. Am. Chem. Soc.* **1998**, *120*, 9053.
(23) Solà, M.; Mestres, J.; Carbó, R.; Duran, M. *J. Am. Chem. Soc.* **1994**, *116*, 5909.
(24) Solà, M., Toro-Labbé, A., *J. Phys. Chem. A* **1999**, *103*, 8847.
(25) Torrent, M.; Duran, M.; Solà, M. *J. Mol. Struct.* (*THEOCHEM*) **1996**, *362*, 163.
(26) Solà, M.; Gonzalez, C.; Tonachini, G.; Schlegel, H. B. *Theor. Chim. Acta* **1990**, *77*, 281. Goumri, A.; Rocha, J. D. R.; Laakso, D.; Smith, C. E.; Marshall, P. *J. Chem. Phys.* **1994**, *101*, 9405.

(27) Hase, W. L. *Science* **1994**, *266*, 998. Glukhotsev, M. N.; Pross, A.; Radom, L. *J. Am. Chem. Soc.* **1996**, *118*, 6273. Wang, H.; Hase, L *J. Am. Chem. Soc.* **1997**, *119*, 3093. Tachikawa, H.; Igarashi, M. *Chem. Phys. Lett.* **1999**, *303*, 81.

(28) Clavero, C.; Lledós, A.; Duran, M.; Ventura, O. N.; Bertrán, J *J. Am. Chem. Soc.* **1986**, *108*, 923. Clavero, C.; Lledós, A.; Duran, M.; Ventura, O. N.; Bertrán, J *J. Comput. Chem.* **1987**, *8*, 481. Solà, M.; Lledós, A.; Duran, M.; Bertrán, J.; Ventura, O. N. *J. Comput. Chem.* **1990**, *11*, 170. Menéndez, M. I.; Suárez, D.; Sordo, J. A.; Sordo, T. L. *J. Comput. Chem.* **1995**, *16*, 659. Toto, J. L.; Pritchard, G. O.; Kirtman, B. *J. Phys. Chem.* **1994**, *88*, 2111. Minyaev, R. M.; Wales, D. J. *Chem Phys. Lett.* **1994**, *218*, 413.

(29) Houk, K. N.; Li, Y.; Slorer, J.; Raimondi, L.; Beno, B. *J. Chem. Soc., Faraday Trans.* **1990**, *90*, 1599. Bernardi, F.; Celani, P.; Olivucci, M.; Robb, M. A.; Suzzi-Valli, G. *J. Am. Chem. Soc.* **1995**, *117*, 10531. Barone, V.; Arnaud, R. *Chem. Phys. Lett.* **1996**, *251*, 393; Barone, V.; Arnaud, R. *J. Chem. Phys.* **1997**, *106*, 8727. Morao, I.; Cossío, F. P. *J. Org. Chem.* **1999**, *64*, 1868. Sakai, S. *J. Phys. Chem. A* **2000**, *104*, 922.

(30) Herges, R.; Jiao, H.; Schleyer, P. v. R. *Angew. Chem., Int. Ed. Eng.* **1994**, *33*, 1376. Jiao, H.; Schleyer, P. v. R. *J. Phys. Org. Chem.* **1998**, *11*, 655.

(31) Gonzalez, C.; Schlegel, H. B. *J. Chem. Phys.* **1988**, *90*, 2154.

(32) Biegler-König, F. W.; Bader, R. F. W.; Tang, T.-H. *J. Comput. Chem.* **1982**, *3*, 317.

(33) Schmidt, M. W.; Baldridge, K. K.; Boate, J. A.; Elbert, S. T.; Gordon, M. S.; Jensen, J. H.; Koseki, S.; Matsunaga, N.; Nguyen, K. A.; Su, S. S.; Windus, T. L.; Dupuis, M.; Montgomery, J. A. GAMESS *J. Comput. Chem.* **1993**, *14*, 1347.

(34) Krishan, R.; Binkley, J. S.; Seeger, R.; Pople, J. A. *J. Chem. Phys.* **1980**, *72*, 650. Clark, T.; Chandreshakar, J.; Spitznagel, G. W.; Schleyer, P. v. R. *J. Comput. Chem.* **1983**, *4*, 294. Frisch, M. J.; Pople, J. A.; Binkley, J. S. *J. Chem. Phys.* **1984**, *80*, 3265.

(35) Frisch, M. J.; Trucks, G. W.; Schlegel, H. B.; Scuseria, G. E.; Robb, M. A.; Cheeseman, J. R.; Zakrzewski, V. G.; Montgomery, J. A.; Stratmann, R. E.; Burant, J. C.; Dapprich. S.; Milliam, J. M.; Daniels, A. D.; Kudin, K. N.; Strain, M. C.; Farkas, O.; Tomasi, J.; Barone, V.; Cossi, M.; Cammi, R.; Mennucci, B.; Pomelli, C.; Adamo, C.; Clifford, S.; Ochterski, J.; Petersson, G. A.; Ayala, P. Y.; Cui, Q.; Morokuma, K.; Malick, D. K.; Rabuck, A. D.; Raghavachari, K.; Foresman, J. B.; Cioslowski, J.; Ortiz, J. V.; Stefanov, B. B.; Liu, G.; Liashenko, A.; Piskorz, P.; Komaromi, I.; Gomperts, R.; Martin, R. L.; Fox, D. J.; Keith, T. A.; Al-Laham, M. A.; Peng, C. Y.; Nanayakkara, A.; Gonzalez, C.; Challacombe, M.; Gill, P. M. W.; Johnson, B. G.; Chen, W.; Wong, M. W.; Andres, J. L.; Head-Gordon, M.; Replogle, E. S.; Pople, J. A. Gaussian Inc., Pittsburgh, PA, 1998.

(36) Actual calculations show that the separation of *core* and valence electrons can be done with errors less than 0.005 electrons for all the λ and δ indices.

(37) For the benzene molecule, which can be considered a typical aromatic molecule, δ(C, C) values are 1.39, 0.07 and 0.10, for C atoms in ortho, meta, and para, respectively, at the HF/6-311++G(2d, 2p) level (see ref 9).